NeuroImage: Clinical 1 (2012) 106–115

Contents lists available at ScienceDirect

NeuroImage: Clinical

journal homepage: www.elsevier.com/locate/ynicl

Brain connectivity and postural control in young traumatic brain injury patients: A diffusion MRI based network analysis☆,☆☆

K. Caeyenberghs [a,*], A. Leemans [b], C. De Decker [a], M. Heitger [a], D. Drijkoningen [a], C. Vander Linden [c], S. Sunaert [d], S.P. Swinnen [a,e]

[a] Motor Control Laboratory, Research Center for Movement Control and Neuroplasticity, KU Leuven, Belgium
[b] Image Sciences Institute, University Medical Center Utrecht, Utrecht, The Netherlands
[c] Child Rehabilitation Centre, Department of Physical Medicine and Rehabilitation, Ghent University Hospital, Belgium
[d] Department of Radiology, University Hospital, KULeuven, Belgium
[e] Leuven Research Institute for Neuroscience & Disease (LIND), KU Leuven, Belgium

ARTICLE INFO

Article history:
Received 29 July 2012
Received in revised form 15 September 2012
Accepted 20 September 2012
Available online 2 October 2012

Keywords:
Diffusion tensor imaging
Graph theoretical network analysis
Motor control
Structural network
Traumatic brain injury
Postural control

ABSTRACT

Our previous research on traumatic brain injury (TBI) patients has shown a strong relationship between specific white matter (WM) diffusion properties and motor deficits. The potential impact of TBI-related changes in network organization of the associated WM structural network on motor performance, however, remains largely unknown. Here, we used diffusion tensor imaging (DTI) based fiber tractography to reconstruct the human brain WM networks of 12 TBI and 17 control participants, followed by a graph theoretical analysis. A force platform was used to measure changes in body posture under conditions of compromised proprioceptive and/or visual feedback. Findings revealed that compared with controls, TBI patients showed higher betweenness centrality and normalized path length, and lower values of local efficiency, implying altered network organization. These results were not merely a consequence of differences in number of connections. In particular, TBI patients displayed reduced structural connectivity in frontal, parieto-premotor, visual, subcortical, and temporal areas. In addition, the decreased connectivity degree was significantly associated with poorer balance performance. We conclude that analyzing the structural brain networks with a graph theoretical approach provides new insights into motor control deficits following brain injury.

1. Introduction

Traumatic brain injury (TBI) is a common cause of disability in children and adolescents worldwide (Kraus and McArthur, 1996), and has a dramatic impact on the developing brain. Besides neurobehavioral and cognitive deficits, TBI results in motor disorders including instability during postural control and gait, which can severely affect the child's level of independence and can increase the risk of falls. Up to 70% of children, who sustain a TBI, present some balance deficits (Black et al., 2000).

Our previous studies in TBI patients have related motor functioning to different structural and functional properties of the brain. Using fMRI, increased recruitment of neural resources for attentional deployment and somatosensory processing was found in children with TBI during motor coordination tasks (Caeyenberghs et al., 2009). It was hypothesized that these modified recruitment patterns might compensate for diffuse axonal injuries (DAI) and disruptions of white matter (WM) connections. Another functional imaging study in adults with TBI (Leunissen et al., 2012) revealed that the neural circuitry supporting motor switching was altered after TBI and that this altered functional engagement was related to behavioral performance across TBI patients and controls. Finally, diffusion tensor imaging (DTI) studies of our group have shown reduced fractional anisotropy values in the whole brain and specific tracts and regions. These studies demonstrated significant correlations between DTI metrics and fine (manual dexterity) and gross (postural control) motor performance, such that increased WM pathology predicts larger motor deficits in children with TBI (e.g., Caeyenberghs et al., 2010a,b, 2011).

Despite these advances in TBI research, however, little is known about the abnormalities in topological organization of brain networks in TBI and whether these are related to motor deficits. Graph theoretical analysis provides a powerful tool to characterize the topological organization of complex networks, and has recently been applied to

☆☆ Funding: This work was supported by a grant from the Research Programme of the Research Foundation-Flanders (FWO) (G.0482.010 and G.A114.11) and Grant P6/29 from the Interuniversity Attraction Poles program of the Belgian federal government. Caeyenberghs K. is funded by a postdoctoral fellowship of the Research Foundation-Flanders (FWO).

* Corresponding author at: Laboratory of Motor Control, Research Center for Motor Control and Neuroplasticity, Group Biomedical Sciences, K.U.Leuven, Tervuursevest 101, B-3001 Heverlee, Belgium. Tel.: 32 16 32 91 14.
E-mail address: Karen.Caeyenberghs@UGent.be (K. Caeyenberghs).

2213-1582/$ – see front matter © 2012 The Authors. Published by Elsevier Inc. All rights reserved.
http://dx.doi.org/10.1016/j.nicl.2012.09.011

the study of human brain networks in health and disease (Bullmore and Sporns, 2009). With respect to TBI, only a few studies have demonstrated small-world alterations and increased connectivity in functional brain networks (Caeyenberghs et al., 2012; Castellanos et al., 2011; Nakamura et al., 2009). To our knowledge, no studies have reported TBI-related changes in the topological properties of WM structural networks. Here, we present the first study using DTI tractography combined with such a graph theoretical approach to investigate the network organization of the WM networks in young patients with TBI and healthy controls.

The present study was based on two main hypotheses:

(i) Relying on our previous study on network functionality in TBI adults (Caeyenberghs et al., 2012), we expected a decrease in structural connectivity in the WM networks. We suggest that higher functional connectivity (i.e., a higher synchronization between activity levels across neural network nodes) may be directly related to a poorer neurobiological substrate, i.e., structural disconnection between areas. As described above, TBI is associated with WM abnormalities that might disrupt neuronal connections. This hypothesis included the consideration that brain injury will not only alter existing structural connections but will also result in a decrease of number of edges between brain areas. This will manifest in measurable changes in mean graph-theoretical network measures when assessing overall network connectivity. Therefore, we sought to determine here whether TBI patients would show abnormal small-world organization, reduced network efficiency and altered nodal efficiency in WM networks.

(ii) Furthermore, we expected a relation between the degree of network connectivity and motor performance in patients with TBI, whereby decreased connectivity degree would be associated with poorer balance. We focused on postural control because this task is a prototype of complex sensorimotor integration, requiring exchange of information among several brain areas.

2. Materials and methods

2.1. Participants

Twenty-nine children and adolescents participated in the study, including 12 subjects with TBI (mean age 14.8 years, SE 1 year 1 month, range 8–20 years of age, seven boys and five girls) and 17 controls (mean age 12.4 years, SE 6 months, range 9–16 years of age; nine boys and eight girls). The TBI patients were classified as 'moderate-to-severe' based on several factors: the Glasgow Coma Scale score after resuscitation (a subgroup of five children had a GCS of 8 or below), the anatomical features of the injury based on inspection by an expert neuroradiologist (see below), and the injury mechanism (traffic accidents and falls), or combinations thereof. The demographic and clinical characteristics of the TBI group are shown in Table 1. The TBI patients were recruited from different rehabilitation centers in Belgium. All were assessed at least six months post-injury, when neurological recovery was stabilized. The interval between injury and scanning (age of injury) was on average 3 years, 6 months (SE 9 months). Their age at injury was on average 10 years, 6 months (SE 3 years, 2 months). Participants were excluded if they had pre-existing developmental or intellectual disabilities, a progressive disease, or were taking medication. All control subjects were screened to ensure that they had no history of neurological damage.

2.2. Posturography

The equipment, paradigm parameters, and dependent variables were identical to our previous DTI study in typically developing children and children with brain injury (Caeyenberghs et al., 2010a). Specifically, the Sensory Organization Test (SOT) of the EquiTest System (Neurocom International Inc.) was used in this study. The equilibrium score indicating postural stability compared the subject's sway to the theoretical limits of stability. The subject's sway was calculated from the maximum anterior and posterior center of gravity (COG) displacements occurring over the 20-s trial period. The theoretical maximum displacement without losing balance was assumed to be a range of 12.5° (6.25 anterior, 6.25 posterior). The results were expressed as percentages, 0 indicating sway exceeding the limit of stability and 100 indicating perfect stability.

The equilibrium score was examined with 4 different sensory conditions (see Fig. 1). In condition A, when the participant stood on a fixed platform with the eyes open, all three sensory systems (vision, vestibular, and somatosensory) were operational and a baseline measure of stability was obtained. Condition B was the same as condition A but with eyes closed. In condition C, the participant stood with the eyes open and the platform moved in response to his/her sway such that the ankle joints did not bend in response to the sway, which reduced proprioceptive input to the brain. Condition D was identical to condition C except that the eyes were now closed, such that only the vestibular system provided reliable sensory information. The test protocol consisted of three repetitions of each condition, resulting in 12 trials. A composite equilibrium score, describing a person's overall level of performance during all the SOT trials was also calculated, with higher scores being indicative of better balance performance.

2.3. MRI data acquisition

MR examination took place without sedation on a 3 T scanner (Intera, Philips, Best, The Netherlands) with an eight channel phased-array head coil. A DTI SE-EPI (diffusion weighted single shot spin-echo echoplanar imaging) was acquired with data acquisition matrix = 112×112; field of view (FOV) = 220×220 mm^2; TR = 7916 ms, TE = 68 ms, parallel imaging factor 2.5, and 68 contiguous sagittal slices (slice thickness = 2.2 mm; voxel size = $2 \times 2 \times 2.2$ mm^3) covering the entire brain and the brainstem (Jones and Leemans, 2011). Diffusion gradients were applied along 45 non-collinear directions with a b-value of 800 s/mm^2. Additionally, one set of images with no diffusion weighting (b = 0 s/mm^2) was acquired.

A T1-weighted coronal 3D-TFE (182 contiguous coronal slices covering the whole brain and brainstem; FOV = 250 mm; TE = 4.6 ms; TR = 9.7 ms; slice thickness = 1.2 mm; matrix size = 256×256; voxel size = $0.98 \times 0.98 \times 1.2$ mm^3) was consequently acquired for anatomical detail (Table 1). These structural MRI scans were investigated by an expert neuro-radiologist to indicate location and type of pathology (e.g., gliosis, shearing, haemorrhage) (see Table 1).

2.4. DTI preprocessing

The DTI data were analyzed and processed in ExploreDTI (Leemans et al., 2009), as described previously (Caeyenberghs et al., 2010a,b, 2011): (a) subject motion and eddy-current induced geometrical distortions were corrected (Leemans and Jones, 2009), and (b) the diffusion tensors were calculated using a non-linear regression procedure (Basser and Pierpaoli, 1996).

2.5. White matter tractography

For each individual dataset, WM tracts of the brain network were reconstructed using a deterministic streamline fiber tractography approach (Basser et al., 2000). Fiber pathways were reconstructed by defining seed points distributed uniformly throughout the data at 2 mm isotropic resolution and by following the main diffusion direction (as defined by the principal eigenvector) until the fiber

Table 1
Summary of demographic and injury characteristics for the TBI group.

TBI patient # Age/gender/ handedness	GCS	Acute scan within 24 h after injury Lesion location/pathology	MRI scan at examination Lesion location/pathology
TBI 1 15,7/F/RH	8	(R) FL subdural hematoma	(R) FL, splenium corpus callosum shearing injuries
TBI 2 9,9/F/RH	5	(R) TL/PL subdural hematoma and (R) cerebellar contusion	(R) TL/PL subdural hematoma and (R) cerebellar contusion
TBI 3 13,1/M/LH		Lesion and location not specified in available records	Hemosiderin deposits (R) thalamus and (R) posterior limb of the internal capsule, shearing injuries corpus callosum
TBI 4 16,6/M/RH	7	Enlarged (R) lateral ventricle, (R) hematoma occipital horn lateral ventricle, hyperdensity (L) thalamus, (LH) shearing injuries	Enlarged (R) lateral ventricle, (RH) atrophy, hemosiderin deposits (splenium corpus callosum, (R) corona radiata), asymmetry cerebral peduncles, (L) contusion pons
TBI 5 14,1/F/RH	3	(R) FL/PL/OL contusion; contusion basal ganglia (thalamus, (R) nucleus caudatus)	Atrophy (R) FL/TL, nucleus caudatus, lentiformis, thalamus, internal capsule, atrophy (R) amygdala, hippocampus, cerebellum; asymmetry lemniscus, cerebral peduncles, pons; shearing injuries corpus callosum
TBI 6 16,8/M/RH	8	(L) TL contusion, (L) FL punctiform contusion, (R) contusion mesen cephalon, (L) FL hemorrhagic injuries and (L) thalamus	Enlarged ventricles, (L) FL hemosiderin deposits
TBI 7 19,1/M/RH		Lesion and location not specified in available records	Shearing injury splenium corpus callosum
TBI 8 20,4/M/RH		(R) FL hematoma, enlarged ventricles	Atrophy RH, (R) contusion superior frontal gyrus, atrophy (R) nucleus caudatus, (R) nucleus lentiformis, injured corpus callosum
TBI 9 17,2/M/RH		Contusions (L) FL, TL, (R) PL, subdural hematoma	Contusion (L) PL inferior, (L) LH hemosiderin deposits, (R) TL contusion, atrophy (L) lateral TL, atrophy (L) FL
TBI 10 11,5/F/RH		(R) FL subdural hematoma, hemorrhagic injuries thalamus, fornix, corpus callosum	(R) FL subdural hematoma
TBI 11 18,7/F/RH		Enlarged ventricles, atrophy PL, FL, RH WM, atrophy (L) hippocampus, shearing injuries	Enlarged ventricles, atrophy LH, (L) PL inferior contusion, injuries superior frontal sulcus, contusion RH, orbitofronal contusion, (R) nucleus lentiformis contusion, asymmetry cerebral peduncles, atrophy (R) cerebellum
TBI 12 8,9/M/RH		Hemorrhagic injuries RH/LH, FL/TL contusion, (L) FL subdural hematoma	(L) FL contusion and subdural hematoma, (R) TL contusion and subdural hematoma

Anatomy codes: WM = white matter; GM = gray matter; RH = right hemisphere; LH = left hemisphere; FL = frontal lobe; TL = temporal lobe; PL = parietal lobe; OL = occipital lobe; R = right; L = left. Other codes: TBI = traumatic brain injury; GCS, Glasgow Coma Scale score; MRI = magnetic resonance imaging; RH = right-handed; LH = left-handed; M = male; F = female.

tract entered a voxel with FA<0.20 or made a high angular turn (angle>45°) considered to be not anatomically plausible. The step size was set at 1 mm.

2.6. Network construction

The whole-brain fiber tract reconstructions of the previous step were parcellated using the automated anatomical labeling atlas (AAL, Tzourio-Mazoyer et al., 2002). This procedure of defining the nodes has been previously described in Bassett et al. (2011a). Using this procedure, we obtained 116 cortical, subcortical and cerebellar regions (58 for each hemisphere), each ROI of the AAL template representing a node of the network (see Figs. 2 and 3), and the edges between two nodes v and u reflecting a reconstructed WM tract.

Inter-regional connectivity was then examined by determining the connection density (number of fiber connections per unit surface) between any two masks (i.e. any two regions of the AAL template) (Hagmann et al., 2008). This value became the edge weight $w(e)$ in an N×N connectivity matrix and was calculated as follows:

$$w(e) = \frac{2}{S_v + S_u} \sum_{f \in F_e} \frac{1}{l(f)}$$

where S_v and S_u denote the cortical surfaces of AAL regions v and u, respectively. F_e denotes the set of all fibers connecting regions v and u and hence contributing to the edge e, and $l(f)$ denotes the length of fiber f along its trajectory. This correction term $l(f)$ in the denominator was needed to eliminate the bias towards longer fibers introduced by the tractography algorithm. Moreover, the sum $S_v + S_u$ corrects for the variable size of the cortical ROIs of the AAL template (Hagmann et al., 2008).

In the main analysis, a weighted graph approach was used. To test the role of the weighting on possible organizational differences between the brain networks of patients and healthy controls, an additional test was performed in which the weighting was omitted from the analysis. For each individual dataset, all nonzero weights (i.e., all connections) were set to 1 and to 0 otherwise (van den Heuvel et al., 2010). The end result of this procedure was an unweighted binary network. As a result, for each participant, there were 2 different kinds of WM networks (density-weighted and binary), each of which was represented by a symmetric 116×116 matrix.

2.7. Graph theory analysis

We investigated the properties of the structural network at the global and regional (nodal) levels using the Brain Connectivity Toolbox (Rubinov and Sporns, 2010, https://sites.google.com/a/brain-connectivity-toolbox.net/bct/), quantifying the global network architecture in terms of small-worldness, normalized clustering coefficient, normalized path length, and global efficiency. We described the regional properties in terms of strength, local efficiency, and betweenness centrality. Based on the constructed structural network, we looked for significant differences in global and nodal properties between the TBI children and controls. In the Supplemental material, we only provide brief, formal definitions of each of the network properties used in this study. For more details and in-depth discussion of these metrics, the interested reader is referred to Rubinov and Sporns (2010).

2.8. Density of structural networks

It has been shown that manipulating the connection density (the number of edges) in a network by varying the number of valid

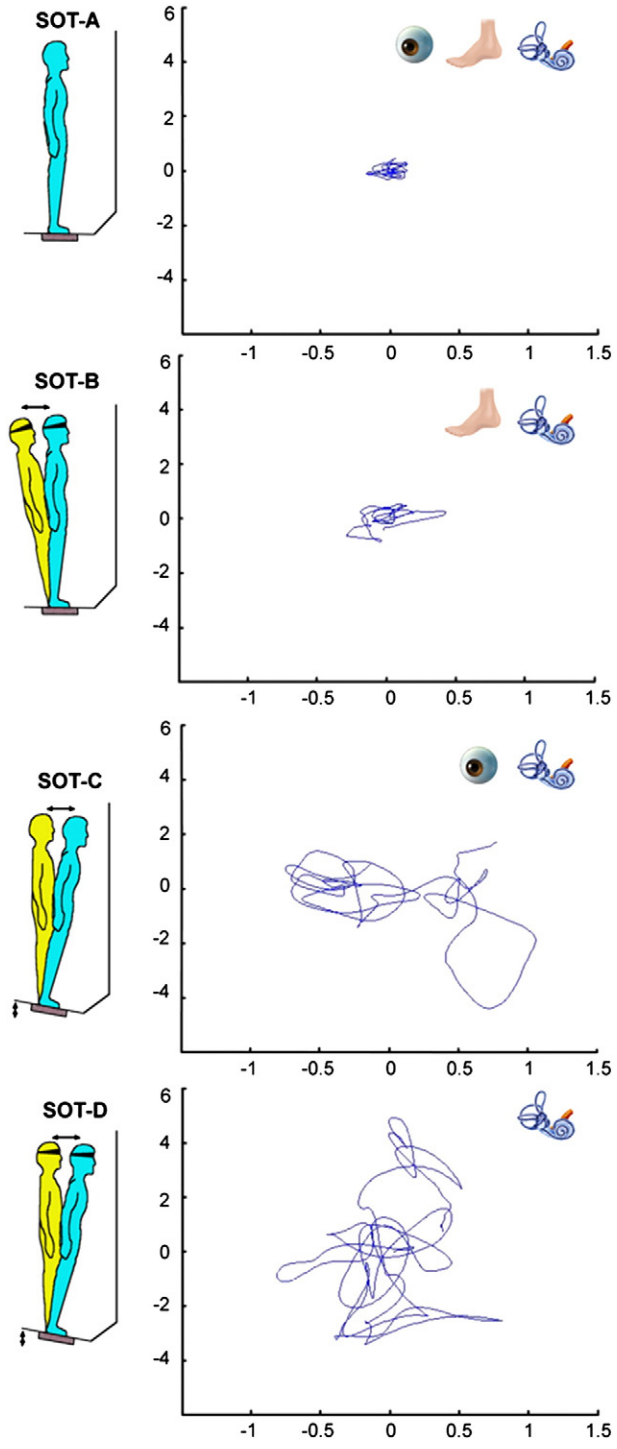

Fig. 1. Schematic representation of the 4 conditions of the Sensory Organization Test and an example data set of a TBI subject's center of pressure (COP) displacement (cm) in anterior–posterior (AP) (y-axis) and medio-lateral (ML) (x-axis) direction across a 20-s trial. In the top right corner of the graphs the status of the sensory systems (visual, proprioceptive, or vestibular) is indicated. Adapted with the permission of Neurocom International, Inc., Clackamas, OR, USA.

network connections can have a noticeable impact on graph-theoretical metrics (Van Wijk et al., 2010). For example, local efficiency has a propensity for being higher with greater numbers of edges in the graph. Hence, we will report differences in graph-theoretical measures, while the wiring cost of a network is taken into account, to ensure that the statistical results with regards to between-group differences in small-world topology and structural connectivity are not simply due to differences in number of connections.

Moreover, in order to be able to compare topological features/aspects of network architecture within a network, it is deemed essential to keep the connection density of the compared networks constant (Van Wijk et al., 2010). However, the underlying hypothesis of this study postulates that TBI is associated with alterations in network organization in the brain, i.e., a lower structural connectivity across the brain areas in the networks will be expressed in a lower number of connections in the TBI group. In order to capture and quantify this aspect of brain injury, we did not enforce the same connection density in our networks for both groups. Consistent with this compromise, we will report changes in the mean graph-theoretical metrics across each entire network but we will not assess specific aspects of network architecture.

2.9. Statistical analysis

The equilibrium scores were subjected to analysis of variance for repeated measurements with between-subjects factor 'group' (2 levels: TBI and control) and the within-subjects factors 'proprioceptive feedback' (2 levels: normal or sway-referenced) and 'visual feedback' (2 levels: normal or abscent). For the composite equilibrium score, two-sample t-tests were conducted for comparing the TBI with the control group.

The number of edges (density) was analyzed using an analysis of covariance (with the effect of age removed) for comparing the TBI with the control group. Statistical comparisons of all network measures (i.e., small worldness, normalized path length, normalized clustering coefficient, strength, local efficiency, and betweenness centrality) between the two groups were performed by means of analyses of covariance (with the effect of density and age removed).

Furthermore, we investigated the regions which showed significant differences in local efficiency. Bonferroni corrections for multiple comparisons were made, hence $p<0.008$ was considered significant following correction for the between-group comparisons regarding the 6 network metrics and $p<0.00043$ for the node-specific analyses regarding the 116 ROIs.

To determine whether the network organization in TBI was correlated with performance on the postural tasks, we calculated partial Pearson's correlation coefficients (with the effect of age removed) of network parameters against the behavioral parameters (4 equilibrium scores and composite equilibrium score). Finally, we conducted region-specific partial correlation analyses between the network metrics and behavioral performance. As described in our previous study (Caeyenberghs et al., 2012), only correlations below a statistical significance level of $p<0.01$ were considered significant. Because of the lack of hemispheric differences (as determined by a p-value >0.05), the right and left hemisphere were combined in these analyses.

Important to note, no significant effect of gender was found in our analyses (all p-values >0.05). Therefore, all the statistical analyses were conducted without this variable as a potential confounding factor. All statistical analyses were performed with the Statistica software (StatSoft, Inc).

3. Results

3.1. Group differences in postural control

Repeated measures analysis of variance showed a significant main effect of group [$F(1,22)=7.21$, $p<0.01$], proprioceptive feedback [$F(1,22)=148.89$, $p<0.001$], and visual feedback [$F(1,22)=261.10$, $p<0.001$], i.e. balance performance was worse (lower equilibrium score) in the TBI versus the control group, when proprioceptive feedback was sway-referenced versus normal and when vision was absent versus normal (as shown in Fig. 4). Furthermore, there was a

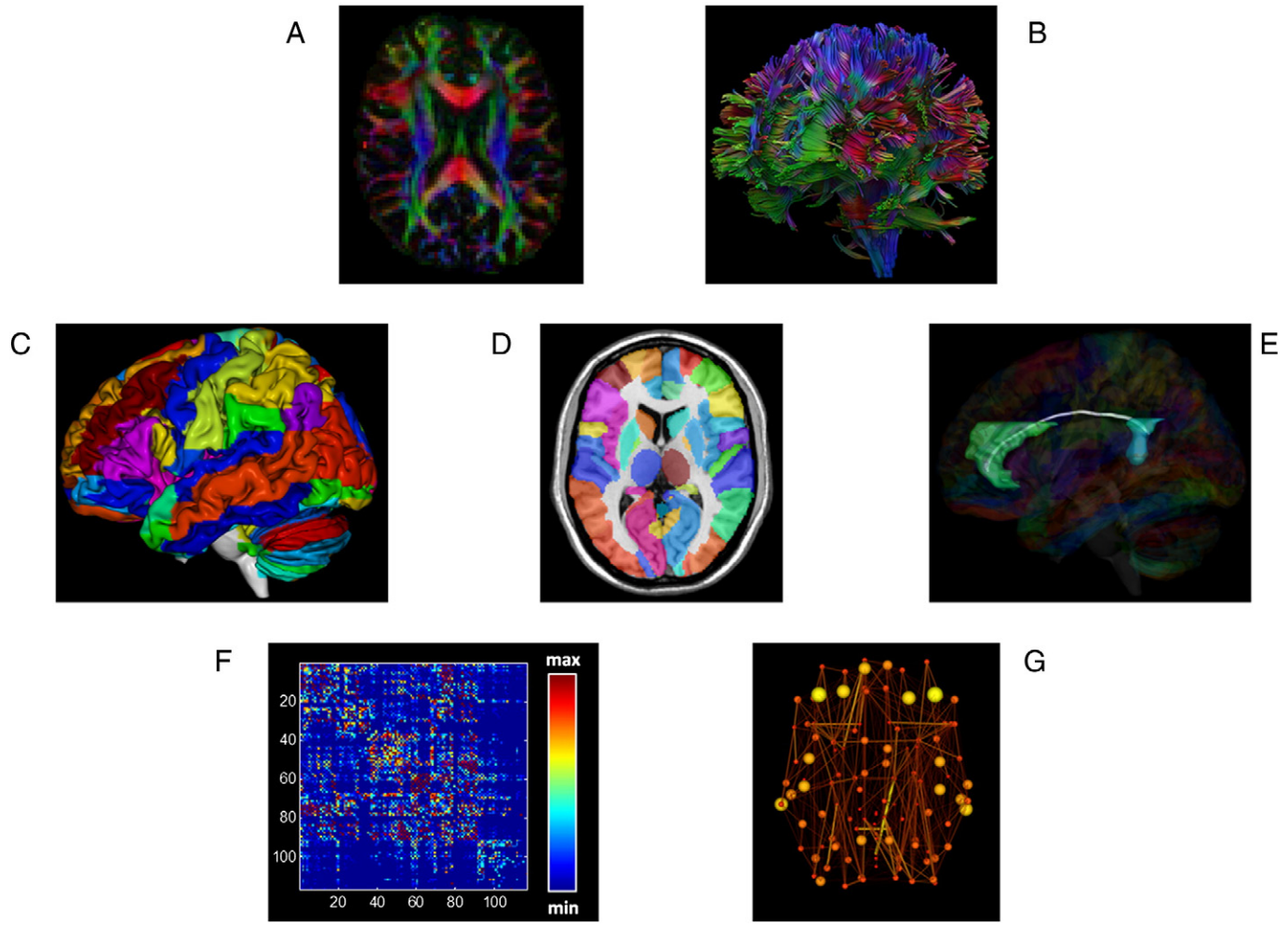

Fig. 2. Flow chart of constructing a DTI-based network. First, for each DTI dataset (A) whole brain deterministic tractography (B) was performed using ExploreDTI (see Materials and methods). The voxel-based reconstruction was then parcellated using the AAL template consisting of 118 unique brain regions (C-D). Fig. 1D shows the AAL labels overlayed on the T1 single subject template provided by MRIcroN. Fig. 1E shows an example of cortical connections and their corresponding WM fibers, linking the right anterior cingulum with the right posterior cingulum. We next determined the number of connections per unit surface between any two masks (any two regions of the AAL template), this value became the edge weight in an 116×116 connectivity matrix (F). Alternatively, an unweighted network analysis was performed, whereby we considered the existence/absence of connections, creating a binary matrix, in which the network edges were defined as 1 if there was at least one connection between both regions and as 0 otherwise. Next, from the resulting brain network (G) overall organizational characteristics and node-specific organizational characteristics were computed and compared between patients and healthy controls.

significant interaction effect between proprioceptive feedback and visual feedback, $F(1,22) = 7.21$, $p<0.01$. Post hoc (Tukey) testing revealed that all participants showed more sway when proprioceptive feedback was compromised, and that sway additionally increased when vision was absent (all p's<0.001). Omission of vision alone did not have a significant effect on balance. Finally, the interaction between proprioceptive feedback and group was also significant, $F(1,22) = 6.62$, $p<0.05$. Post hoc (Tukey) testing showed that the TBI group performed significantly worse than the controls on the sway-referenced conditions (all p's<0.001). Moreover, post hoc Tukey tests revealed significant differences between normal and sway-referenced feedback within each group (all p's<0.001).

The mean composite SOT balance score (average across all four conditions) from the Equitest system also differed significantly between the TBI patients (mean = 67.1%; range 46.3–84.0%) and the controls (mean = 77.0%; range 66.6–82.7%), $t(22) = -2.69$, $p<0.01$, with the lower scores in the TBI subjects indicating poorer balance (larger anterior/posterior body sway) than in the controls.

3.2. Density of structural brain networks

A significant effect for group was seen on density, representing the total "wiring cost" of the network [$F(1,26) = 46.43$, $p<0.001$]. In other words, the average number of edges was significantly lower in TBI patients (mean = 4857, SD = 2193) compared with controls (mean = 9702, SD = 1254). Therefore, our main analyses regarding between-group differences in small-world topology and structural connectivity were conducted by including density as covariate in each analysis.

3.3. Small-world properties and organization of structural brain networks

3.3.1. Small world topology

The small-world attributes reflect the need of the structural network to satisfy the opposing demands of local and global processing (Kaiser and Hilgetag, 2006). In other words, an optimal brain requires a suitable balance between local specialization, supported by higher absolute clustering coefficients, and global integration, supported by shorter absolute path lengths. This balance of global and local connectivity was abnormally shifted toward the global end of the scale in TBI patients. This could be quantified by a change in the small-worldness parameter σ. Although networks in both groups were small-world ($\sigma>1$), indicating that they had generally greater-than-random clustering ($\gamma>>1$) (TBI group: mean = 5.94, SD = 1.71; control group: mean = 3.88, SD = 0.32), but near-random path length ($\lambda\approx1$) (TBI group: mean = 1.01, SD = 0.06; control group: mean = 1.04, SD =

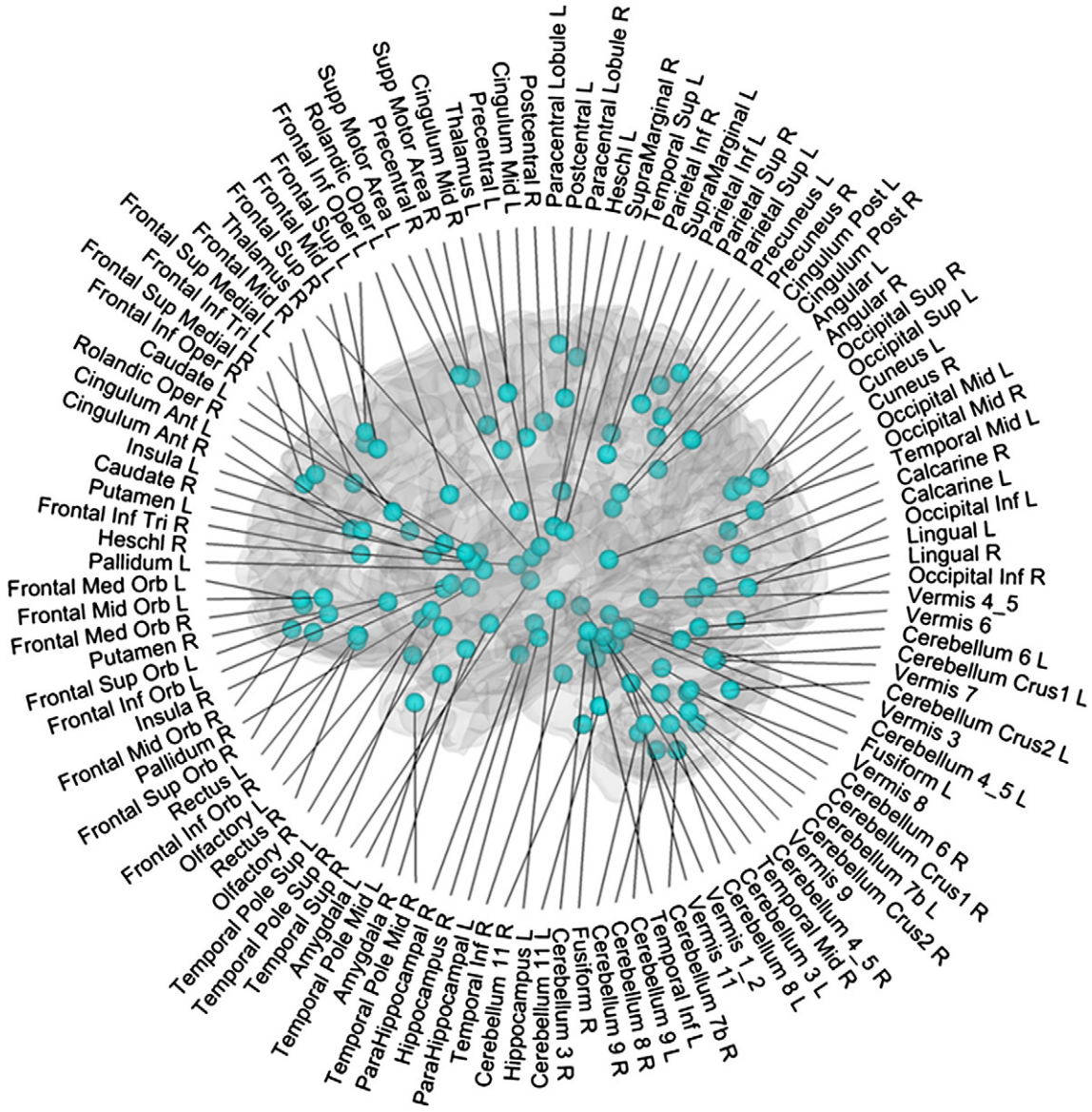

Fig. 3. Cortical and subcortical regions (58 in each hemisphere; 118 in total) as anatomically defined by a prior template image in standard stereotaxic space.

0.02), small-worldness was marginally increased [$F(1,25) = 5.41$, $p < 0.05$] because of the increase in normalized path length [$F(1,25) = 8.66$, $p_{corr} < 0.008$] in the TBI group.

3.3.2. TBI-related alterations in structural connectivity

Using ANOVA's with age and density as covariate, we observed that the TBI group showed decreased values of local efficiency [$F(1,25) = 10.46$, $p_{corr} < 0.008$] in their WM networks as compared to the controls. We further compared the nodal efficiency of (sub)cortical regions in WM networks between the two groups. We found that TBI networks showed decreased local efficiency (all $p_{corr} < 0.00043$) predominantly located in the occipital regions (including the calcarine fissure, left cuneus, lingual gyrus, superior, middle and inferior occipital gyrus), and subcortical regions (including the left olfactory cortex, left caudate nucleus, left putamen, left thalamus, cerebellum Crus I, and right cerebellum Crus II). Additionally, we also found decreased local efficiency (all $p_{corr} < 0.00043$) in frontal regions (the left superior frontal gyrus, orbital part of the left middle frontal gyrus, triangular part of the left inferior frontal gyrus, medial (orbital) part of the superior frontal gyrus, left gyrus rectus, right anterior cingulate gyrus), parietal-(pre)motor regions (i.e., right precentral gyrus, postcentral gyrus, superior parietal gyrus, right supramarginal gyrus, right angular gyrus, left precuneus), and four medial temporal lobe regions (left parahippocampal gyrus, temporal pole of the superior and middle temporal gyrus, left middle temporal gyrus). Node specific values of local efficiency of both groups are presented in Fig. 5.

WM networks of TBI patients showed an increased betweenness centrality compared with controls [$F(1,25) = 7.76$, $p_{corr} < 0.008$]. Furthermore, structural network analysis estimated for TBI and controls revealed that both groups exhibited hubs. In particular, 5 hub regions were shared by both groups, i.e., the bilateral precuneus, right superior frontal gyrus, left middle occipital gyrus, and left thalamus. Of note, three brain regions, the left superior frontal gyrus, right superior parietal gyrus, and right postcentral gyrus, were identified as hubs in the control group but not in the TBI group. Three other brain regions, the left precentral gyrus, right supplementary motor area, and left putamen, were identified as hubs in the TBI group but not in the control group.

3.4. Network properties correlation with postural control

We next examined the relationships between the network metrics and postural control. We considered only connectivity degree as a

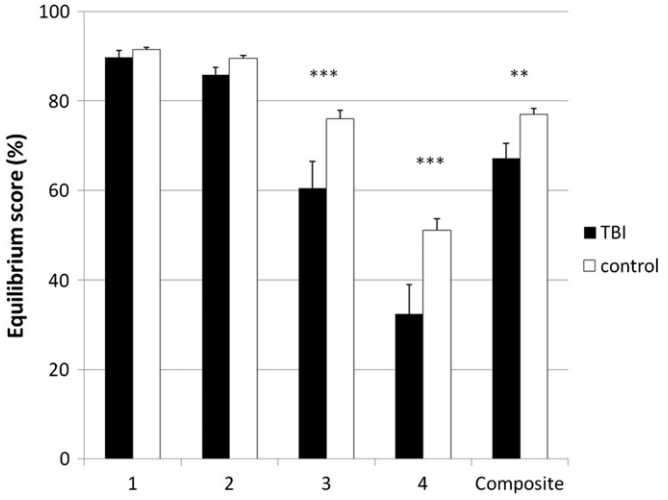

Fig. 4. Behavioral task performance. The TBI group performed significantly worse than the controls on the sway referenced conditions and on the composite balance score. TBI, black bars; control, white bars; $^{**}p<0.01$, $^{***}p<0.001$ for the TBI group compared to controls; TBI, traumatic brain injury.

network property in these analyses because it has been suggested to be the most important measure of network analysis which is also assigned a straightforward neurobiological interpretation (Rubinov and Sporns, 2010): nodes with a high connectivity degree are structurally interacting with many other nodes in the network. Moreover, network degree is most commonly used as a measure of density, or the total "wiring cost" of the network (Rubinov and Sporns, 2010). To determine the relationships, partial correlation analysis with age as confounding covariate were separately performed for the TBI and control groups. In the control group, none of the balance measures showed significant correlations with the network metrics. The following descriptions focus on the results in the TBI group. Fig. 6 shows the significant correlations between balance scores and connectivity degree across the whole network on the one hand and regional connectivity degree on the other hand.

A significant positive correlation was found between mean connectivity degree of the network in the TBI group and mean composite SOT score ($r=0.65$, $p<0.05$). In other words, increase in connectivity degree was associated with better balance performance (i.e., lower anterior/posterior body sway). Significant correlations between connectivity degree across the whole network and equilibrium scores for the separate conditions were only found for the condition where proprioceptive feedback and visual feedback were compromised (condition D), i.e., higher connectivity degree was associated with better performance on the postural task ($r=0.62$, $p<0.05$).

A more stringent threshold criterion ($p_{corr}<0.01$) was used to further determine the associations between specific nodes on one hand and the composite score and equilibrium score of condition D on the other hand. Significant correlations were obtained between the composite score and connectivity degree of the superior parietal gyrus ($r=0.73$, $p_{corr}<0.01$). Also, we found that the equilibrium score of condition D (eyes closed, sway-referenced platform) was significantly positively correlated with connectivity degree of the superior parietal gyrus ($r=0.78$, $p_{corr}<0.01$) and cerebellar lobule IX ($r=0.71$, $p_{corr}<0.01$).

4. Discussion

We compared the WM networks between young TBI patients and healthy controls using DTI tractography and graph theoretical approaches. Both groups exhibited small-world properties in their WM networks. However, efficiency was significantly decreased in the TBI patients compared with controls, with pronounced changes in the frontal, occipital, parieto-premotor, subcortical, and medial-temporal areas. Moreover, connectivity degree was significantly correlated with the balance scores. Our data show disrupted network organization of WM networks in TBI patients, which may contribute to their persistent motor disabilities.

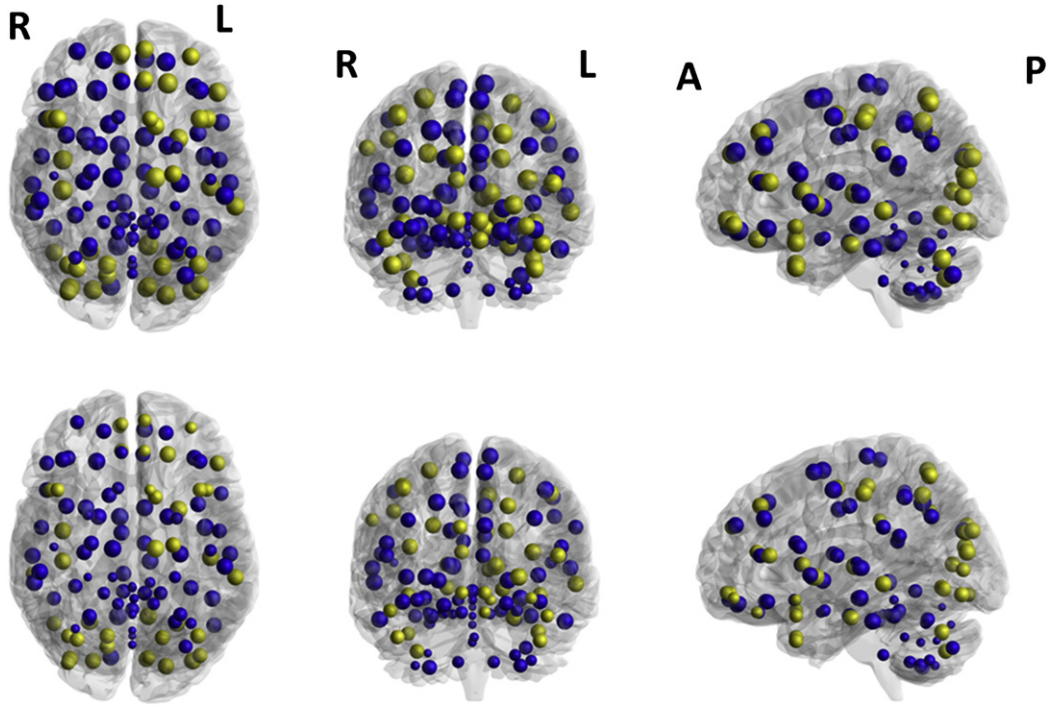

Fig. 5. Group differences in local efficiency. Upper panel: controls, lower panel: TBI patients. Size of the ROIs (spheres) represents the local efficiency. The colors of the nodes refer to: yellow, significant after correction for multiple comparisons, $p<0.0043$; blue, not significant.

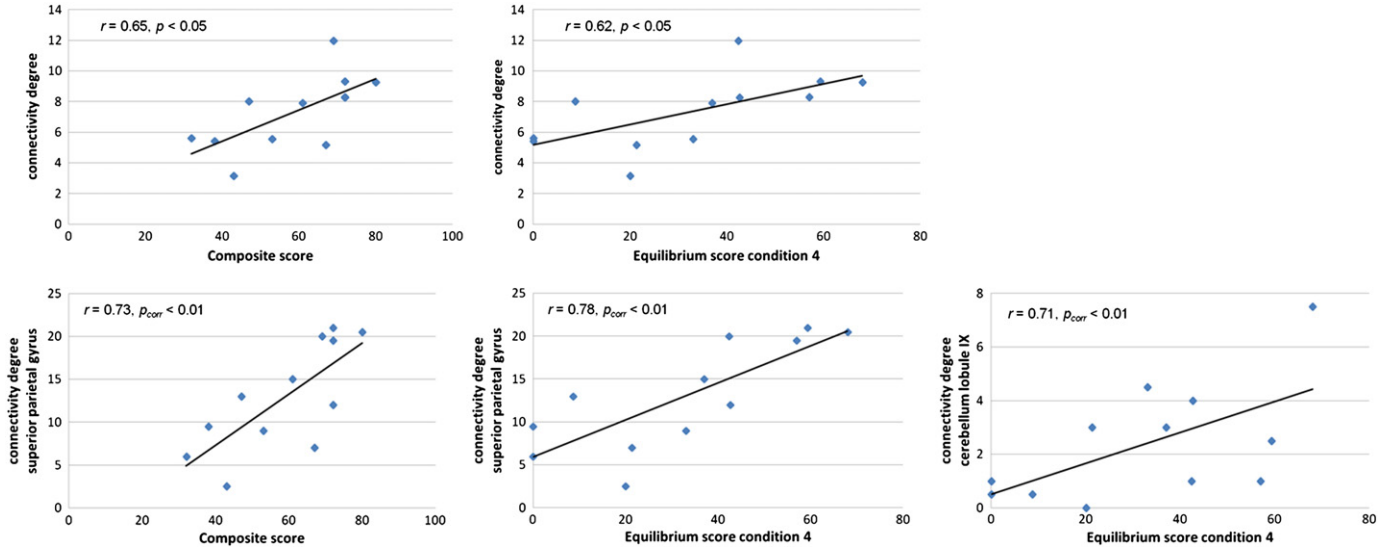

Fig. 6. Plots indicating the relationships between the balance scores (mean composite score and equilibrium score of condition 4) and connectivity degree across the whole network (upper panel) and regional connectivity degree (lower panel).

4.1. Group differences in postural control

Our results suggest that the integration of sensory inputs is disturbed following TBI. In other words, TBI patients showed deficits in selecting the accurate and suppressing the compromised sensory inputs. Lower scores on the SOT have been well documented in TBI patients, especially in conditions where visual and vestibular inputs must be relied upon to produce stability, even in the absence of any clinically detectable neurological problem (Geurts et al., 1996; Guskiewicz et al., 1997). These results are consistent with previous studies using clinical tests of postural control in TBI. For example, abnormally increased sway and reduced time scores during the Clinical Test for Sensory Interaction in Balance have been reported previously (Ingersoll and Armstrong, 1992; Lehmann et al., 1990; Rubin et al., 1995).

4.2. Group differences in structural WM networks

We identified that both TBI patients and controls displayed prominent small-world properties in the WM networks. This finding is consistent with previous structural network studies of the human brain using diffusion tractography in normal adults (Gong et al., 2009; Hagmann et al., 2007, 2008; Iturria-Medina et al., 2008) and in patient populations (Lo et al., 2010; Shu et al., 2009, 2011; van den Heuvel et al., 2010; Wen et al., 2011). We found that, although WM networks of young TBI patients showed prominent small-world properties, several network parameters were found to be significantly altered, such as the normalized path length, local efficiency, and betweenness centrality. Important to note, these differences in network topology were not only due to differences in number of connections.

Compared with the small-world properties of matched random networks, an increased normalized path length (along with a marginal increase in small-worldness) was observed in the TBI group. Given that the small-world topology is an optimal balance between local specialization and global integration as networks evolved over time to cope with high complexity of dynamic behavior (Bullmore and Sporns, 2009), our findings of increased normalized path length and small-worldness in TBI networks indicate a shift away from an optimal 'small world' network organization towards an imbalanced structural architecture with a more random configuration in WM networks.

Furthermore, lower efficiency was found in five distinct systems: frontal, occipital, parieto-premotor, subcortical, and medial-temporal systems. Hence, our data support the notion of TBI as a 'disconnection syndrome' from a network perspective. The observed increased betweenness centrality in the TBI group may indicate a possible compensatory mechanism for decreased structural connectivity.

4.3. Importance of specific brain regions for network functionality

Structural network analyses conducted in TBI and controls revealed that both groups exhibit hubs. In particular, five hub regions were shared by both groups, the bilateral precuneus, right superior frontal gyrus, left middle occipital gyrus, and left thalamus. It is worth noting that the precuneus was identified as the most important region in WM networks of TBIs and controls. The precuneus is part of the posterior parietal cortex which belongs to a widespread network of higher association structures (Cavanna and Trimble, 2006), indicating its central role across a broad spectrum of highly integrative tasks. The precuneus has also been ranked as the most pivotal region in previous diffusion-MRI tractography network analyses in healthy adults (Hagmann et al., 2007; Gong et al., 2009; Shu et al., 2009), and an equivalent region to the precuneus (Brodmann area 7) was also identified as a hub in the macaque cortical network (Sporns et al., 2007).

One brain region, the left putamen, was identified as a hub in the TBI group but not in the control group. The putamen, together with the caudate nucleus, makes up the striatum, a major site of cortical and subcortical input into the basal ganglia as part of a cortico-striatal loop (Alexander et al., 1990). Its role has been implicated in a number of important motor functions (Coghill et al., 1994; Jones et al., 1991), in particular in the initiation of motor responses (Coxon et al., 2010; Toxopeus et al., 2007). Moreover, two other sensorimotor regions, which are implicated in planning of motor actions and bimanual control (including the left precentral gyrus and right supplementary motor area) were also identified as hubs in the TBI group. Although, to the best of our knowledge, no study has so far investigated structural or functional changes in these three regions in TBI patients, we hypothesize that the increased betweenness centrality of these regions in the structural network may be linked to compensatory reorganization aiming to alleviate the reduced capacity for movement initiation in TBI patients.

4.4. Behavioral relevance of network alterations in TBI

Previously unreported, we have now shown associations between motor disabilities and structural brain organization in TBI patients

from a network perspective. Our results indicated that the TBI-related alterations in network properties were associated with balance deficits. We found that young TBI patients with decreased structural connectivity degree in WM networks displayed lower balance performance (i.e. higher anterior/posterior body sway).

Node-specific correlation analyses performed within the TBI group revealed significant correlations between the composite equilibrium score and the equilibrium score of condition 4 on one hand and connectivity degree of a subset of brain regions on the other hand, including cortical regions located in the superior parietal lobule, as well as subcortical structures such as the cerebellar lobule IX.

First, the correlation analyses provided evidence that deficits in postural control are related to lower connectivity degree in the superior parietal lobule. The superior parietal lobule is a major component of a distributed spatial attention network (Pollmann et al., 2003; Vandenberghe et al., 2001; Yantis et al., 2002). More specifically, Molenberghs et al. (2007) have suggested that the function of the superior parietal lobule is closely related to the modification of spatial coordinates linked to attentional priorities (spatial shifting). This is consistent with the notion that the postural control task in our study required seeking and selectively attending to significant extrapersonal stimuli in a dynamic environment, which in turn requires updating the attentional priority map.

Secondly, the equilibrium score of condition D (eyes closed, sway-referenced platform) was also significantly correlated to connectivity degree in subcortical structures, such as lobule IX of the cerebellum. Lobule IX has been implicated in various functional tasks including sensation (Hui et al., 2005), motor synchronization (Jantzen et al., 2004), working memory (Desmond et al., 1997), and perception of change in stimulus timing (Liu et al., 2008). Interestingly, this result is in agreement with our previous DTI study (Caeyenberghs et al., 2010a), showing associations between the SOT balance scores and fractional anisotropy in the cerebellar peduncles and cerebellum. Specifically, performance on condition D was positively related to mean fractional anisotropy in the superior cerebellar peduncle, with better balance being associated with higher WM anisotropy. These results suggest that evaluation of key motor control brain areas such as the cerebellum using DTI tractography combined with a graph theoretical approach could be helpful in developing imaging biomarkers for diagnostics/prognosis in patients with balance deficits following TBI.

All these node-specific results are consistent with the notion that postural control is an extremely complex function that requires the intensive cooperation of cortical and subcortical structures to support intersensory integration for action. Important to note, connectivity degree was not significantly correlated with the other balance conditions. We assume that balance conditions have to be sufficiently challenging (i.e., under deprived sensory conditions) for significant network organization-balance relations to emerge.

4.5. Study limitations and considerations for interpreting the current findings

Limitations of the current study pertain to the relatively small sample size and the cross sectional design. Despite the clear findings, their replication in a larger sample is mandatory. In addition, it has been shown recently that there are many brain regions with complex fiber architecture, also referred to as "crossing fibers" (Jeurissen et al., 2011; Tournier et al., 2011). In these regions, where the diffusion tensor model has been shown to be inadequate (Frank, 2002; Tuch et al., 2002), partial volume effects exist (Alexander et al., 2001; Vos et al., 2011) that can adversely affect the estimation of diffusivity metrics (Wheeler-Kingshott and Cercignani, 2009; Vos et al., 2012). In this context, tractography approaches based on more advanced diffusion models (e.g., Behrens et al., 2007; Descoteaux et al., 2009; Jeurissen et al., 2011) may provide more accurate anatomical connectivity patterns of brain networks.

Our main analyses showed consistent changes in structural connectivity between controls and patients that manifested across multiple graph-theoretical metrics, showing that this decrease in mean structural connectivity could be captured across multiple (albeit inter-related) sub-domains of structural connectivity. However, it has to be emphasized that in the present exploratory analysis the number of network connections was different between the two groups indicating the effect of brain injury in their networks. A disadvantage of having a different number of connections (i.e., not limiting the network connections to a constant number in both groups) in our networks is that we cannot make inferences about specific topological aspects of the networks (see van Wijk et al., 2010). Hence, the present findings do not prove that the reduced structural connectivity in TBI patients is due to significant changes in network topology but might have been carried substantially by a decrease in number of network connections. Including density as a covariate is not sufficient to control for differences in number of edges, because most graph measures are non-linearly dependent on density.

Furthermore, for computational reasons normal theory based test statistics were conducted instead of permutation testing (Ginestet and Simmons, 2011; van Wijk et al., 2010). Correction for multiple comparisons on one hand and correction for density on the other hand were used, but future studies are needed to determine the optimal methodology to control for multiple testing in a network setting and differences in network costs respectively. Alternative correction methods (Zalesky et al., 2010) and formal methods to the comparison of several families of networks (Bassett et al., 2011b; Ginestet et al., 2011) have been suggested. Finally, longitudinal studies are needed to determine how changes in topological structure of WM networks are related to recovery and objective measures of postural control.

4.6. Conclusions

Taking into account these limitations, the present study is the first report illustrating associations between network metrics and postural control scores in a young TBI group. Although small-world properties were present for both patient and control networks, the architecture of the structural networks was significantly altered in TBI patients. Specifically, TBI patients showed decreased connectivity degree, strength, and lower values of local efficiency. Furthermore, the decreased connectivity degree was significantly associated with postural control performance. These brain-behavior relations pave the way for topology-based brain network analyses that may ultimately serve as biomarkers to improve TBI diagnostics/prognosis and for follow-up of balance deficits.

Conflict of Interest

There are no conflicts of interest.

Appendix A. Supplementary data

Supplementary data to this article can be found online at http://dx.doi.org/10.1016/j.nicl.2012.09.011.

References

Alexander, G.E., Crutcher, M.D., DeLong, M.R., 1990. Basal ganglia–thalamocortical circuits: parallel substrates for motor, oculomotor, "prefrontal" and "limbic" functions. Progress in Brain Research 85, 119–146.

Alexander, A.L., Hasan, K.M., Lazar, M., Tsuruda, J.S., Parker, D.L., 2001. Analysis of partial volume effects in diffusion-tensor MRI. Magnetic Resonance in Medicine 45, 770–780.

Basser, P.J., Pierpaoli, C., 1996. Microstructural and physiological features of tissues elucidated by quantitative-diffusion-tensor MRI. Journal of Magnetic Resonance. Series B 111, 209–219.

Basser, P.J., Pajevic, S., Pierpaoli, C., Duda, J., Aldroubi, A., 2000. In vivo fiber tractography using DT-MRI data. Magnetic Resonance in Medicine 44, 625–632.

Bassett, D.S., Brown, J.A., Deshpande, V., Carlson, J.M., Grafton, S.T., 2011a. Conserved and variable architecture of human white matter connectivity. NeuroImage 54, 1262–1279.

Bassett, D.S., Wymbs, N.F., Porter, M.A., Mucha, P.J., Carlson, J.M., Grafton, S.T., 2011b. Dynamic reconfiguration of human brain networks during learning. Proceedings of the National Academy of Sciences of the United States of America 108, 7641–7646.
Behrens, T.E.J., Berg, H.J., Jbabdi, S., Rushworth, M.F.S., Woolrich, M.W., 2007. Probabilistic diffusion tractography with multiple fibre orientations: what can we gain? NeuroImage 34, 144–155.
Black, K., Zafonte, R., Millis, S., Desantis, N., Harrison-Felix, C., Wood, D., Mann, N., 2000. Sitting balance following brain injury: does it predict outcome? Brain Injury 14, 141–152.
Bullmore, E., Sporns, O., 2009. Complex brain networks: graph theoretical analysis of structural and functional systems. Nature Reviews. Neuroscience 10, 186–198.
Caeyenberghs, K., Wenderoth, N., Smits-Engelsman, B.C., Sunaert, S., Swinnen, S.P., 2009. Neural correlates of motor dysfunction in children with traumatic brain injury: exploration of compensatory recruitment patterns. Brain 132, 684–694.
Caeyenberghs, K., Leemans, A., Geurts, M., Taymans, T., Linden, C.V., Smits-Engelsman, B.C., Sunaert, S., Swinnen, S.P., 2010a. Brain–behavior relationships in young traumatic brain injury patients: DTI metrics are highly correlated with postural control. Human Brain Mapping 31, 992–1002.
Caeyenberghs, K., Leemans, A., Geurts, M., Taymans, T., Vander, L.C., Smits-Engelsman, B.C., Sunaert, S., Swinnen, S.P., 2010b. Brain–behavior relationships in young traumatic brain injury patients: fractional anisotropy measures are highly correlated with dynamic visuomotor tracking performance. Neuropsychologia 48, 1472–1482.
Caeyenberghs, K., Leemans, A., Geurts, M., Linden, C.V., Smits-Engelsman, B.C., Sunaert, S., Swinnen, S.P., 2011. Correlations between white matter integrity and motor function in traumatic brain injury patients. Neurorehabilitation and Neural Repair 25, 492–502.
Caeyenberghs, K., Leemans, A., Heitger, M.H., Leunissen, I., Dhollander, T., Sunaert, S., Dupont, P., Swinnen, S.P., 2012. Graph analysis of functional brain networks for cognitive control of action in traumatic brain injury. Brain 135, 1293–1307.
Castellanos, N.P., Leyva, I., Buldu, J.M., Bajo, R., Paul, N., Cuesta, P., Ordonez, V.E., Pascua, C.L., Boccaletti, S., Maestu, F., del-Pozo, F., 2011. Principles of recovery from traumatic brain injury: reorganization of functional networks. NeuroImage 55, 1189–1199.
Cavanna, A.E., Trimble, M.R., 2006. The precuneus: a review of its functional anatomy and behavioural correlates. Brain 129, 564–583.
Coghill, R.C., Talbot, J.D., Evans, A.C., Meyer, E., Gjedde, A., Bushnell, M.C., Duncan, G.H., 1994. Distributed processing of pain and vibration by the human brain. The Journal of Neuroscience 14, 4095–4108.
Coxon, J.P., Goble, D.J., Van Impe, A., De Vos, J., Wenderoth, N., Swinnen, S.P., 2010. Reduced Basal Ganglia Function When Elderly Switch between Coordinated Movement Patterns. Cerebral Cortex 20, 2368–2379.
Descoteaux, M., Deriche, R., Knosche, T.R., Anwander, A., 2009. Deterministic and Probabilistic Tractography Based on Complex Fibre Orientation Distributions. IEEE Transactions on Medical Imaging 28, 269–286.
Desmond, J.E., Gabrieli, J.D.E., Wagner, A.D., Ginier, B.L., Glover, G.H., 1997. Lobular patterns of cerebellar activation in verbal working-memory and finger-tapping tasks as revealed by functional MRI. The Journal of Neuroscience 17, 9675–9685.
Frank, L.R., 2002. Characterization of anisotropy in high angular resolution diffusion-weighted MRI. Magnetic Resonance in Medicine 47, 1083–1099.
Geurts, A.C., Ribbers, G.M., Knoop, J.A., van Limbeek, J., 1996. Identification of static and dynamic postural instability following traumatic brain injury. Archives of Physical Medicine and Rehabilitation 77, 639–644.
Ginestet, C.E., Simmons, A., 2011. Statistical parametric network analysis of functional connectivity dynamics during a working memory task. NeuroImage 55, 688–704.
Ginestet, C.E., Nichols, T.E., Bullmore, E.T., Simmons, A., 2011. Brain Network Analysis: Separating Cost from Topology Using Cost-Integration. PLoS One 6 (7), e21570 (Electronic publication ahead of print 2011 Jul 28).
Gong, G., He, Y., Concha, L., Lebel, C., Gross, D.W., Evans, A.C., Beaulieu, C., 2009. Mapping anatomical connectivity patterns of human cerebral cortex using in vivo diffusion tensor imaging tractography. Cerebral Cortex 19, 524–536.
Guskiewicz, K.M., Riemann, B.L., Perrin, D.H., Nashner, L.M., 1997. Alternative approaches to the assessment of mild head injury in athletes. Medicine and Science in Sports and Exercise 29, S213–S221.
Hagmann, P., Kurant, M., Gigandet, X., Thiran, P., Wedeen, V.J., Meuli, R., Thiran, J.P., 2007. Mapping human whole-brain structural networks with diffusion MRI. PloS One 2, e597.
Hagmann, P., Cammoun, L., Gigandet, X., Meuli, R., Honey, C.J., Wedeen, V., Sporns, O., 2008. Mapping the structural core of human cerebral cortex. PLoS Biology 6, 1479–1493.
Hui, K.K.S., Liu, J., Marina, O., Napadow, V., Haselgrove, C., Kwong, K.K., Kennedy, D.N., Makris, N., 2005. The integrated response of the human cerebro-cerebellar and limbic systems to acupuncture stimulation at ST 36 as evidenced by fMRI. NeuroImage 27, 479–496.
Ingersoll, C.D., Armstrong, C.W., 1992. The Effects of Closed-Head Injury on Postural Sway. Medicine and Science in Sports and Exercise 24, 739–743.
Iturria-Medina, Y., Sotero, R.C., Canales-Rodriguez, E.J., Aleman-Gomez, Y., Melie-Garcia, L., 2008. Studying the human brain anatomical network via diffusion-weighted MRI and Graph Theory. NeuroImage 40, 1064–1076.
Jantzen, K.J., Steinberg, F.L., Kelso, J.A.S., 2004. Brain networks underlying human timing behavior are influenced by prior context. Proceedings of the National Academy of Sciences of the United States of America 101, 6815–6820.
Jeurissen, B., Leemans, A., Jones, D.K., Tournier, J.D., Sijbers, J., 2011. Probabilistic Fiber Tracking Using the Residual Bootstrap with Constrained Spherical Deconvolution. Human Brain Mapping 32, 461–479.
Jones, D.K., Leemans, A., 2011. Diffusion tensor imaging. Methods in Molecular Biology 711, 127–144.
Jones, A.K., Brown, W.D., Friston, K.J., Qi, L.Y., Frackowiak, R.S., 1991. Cortical and subcortical localization of response to pain in man using positron emission tomography. Proceedings. Biological sciences / The Royal Society 244, 39–44.
Kaiser, M., Hilgetag, C.C., 2006. Nonoptimal component placement, but short processing paths, due to long-distance projections in neural systems. PLoS Computational Biology 2, 805–815.
Kraus, J.F., McArthur, D.L., 1996. Epidemiologic aspects of brain injury. Neurologic Clinics 14, 435–450.
Leemans, A., Jones, D.K., 2009. The B-matrix must be rotated when correcting for subject motion in DTI data. Magnetic Resonance in Medicine 61, 1336–1349.
Leemans, A., Jeurissen, B., Sijbers, J., Jones, D.K., 2009. ExploreDTI: a graphical toolbox for processing, analyzing, and visualizing diffusion MR data. In: 17th Annual Meeting of Intl Soc Mag Reson Med. p. 3537, Hawaii, USA.
Lehmann, J.F., Boswell, S., Price, R., Burleigh, A., Delateur, B.J., Jaffe, K.M., Hertling, D., 1990. Quantitative-evaluation of sway as an indicator of functional balance in posttraumatic brain injury. Archives of Physical Medicine and Rehabilitation 71, 955–962.
Leunissen, I., Coxon, J.P., Geurts, M., Caeyenberghs, K., Michiels, K., Sunaert, S., Swinnen, S.P., 2012. Disturbed cortico-subcortical interactions during motor task switching in traumatic brain injury. Human Brain Mapping. http://dx.doi.org/10.1002/hbm.21508 (Electronic publication ahead of print 2012 Jan 30).
Liu, T., Xu, D., Ashe, J., Bushara, K., 2008. Specificity of inferior olive response to stimulus timing. Journal of Neurophysiology 100, 1557–1561.
Lo, C.Y., Wang, P.N., Chou, K.H., Wang, J., He, Y., Lin, C.P., 2010. Diffusion tensor tractography reveals abnormal topological organization in structural cortical networks in Alzheimer's disease. The Journal of Neuroscience 30, 16876–16885.
Molenberghs, P., Mesulam, M.M., Peeters, R., Vandenberghe, R.R.C., 2007. Remapping attentional priorities: Differential contribution of superior parietal lobule and intraparietal sulcus. Cerebral Cortex 17, 2703–2712.
Nakamura, T., Hillary, F.G., Biswal, B.B., 2009. Resting network plasticity following brain injury. PLoS One 4, e8220.
Pollmann, S., Weidner, R., Humphreys, G.W., Olivers, C.N.L., Muller, K., Lohmann, G., Wiggins, C.J., Watson, D.G., 2003. Separating distractor rejection and target detection in posterior parietal cortex — an event-related fMRI study of visual marking. NeuroImage 18, 310–323.
Rubin, A.M., Woolley, S.M., Dailey, V.M., Goebel, J.A., 1995. Postural stability following mild head or whiplash injuries. The American Journal of Otology 16, 216–221.
Rubinov, M., Sporns, O., 2010. Complex network measures of brain connectivity: uses and interpretations. NeuroImage 52, 1059–1069.
Shu, N., Liu, Y., Li, J., Li, Y.H., Yu, C.S., Jiang, T.Z., 2009. Altered anatomical network in early blindness revealed by diffusion tensor tractography. PLoS One 4, e7228.
Shu, N., Liu, Y., Li, K., Duan, Y., Wang, J., Yu, C., Dong, H., Ye, J., He, Y., 2011. Diffusion tensor tractography reveals disrupted topological efficiency in white matter structural networks in multiple sclerosis. Cerebral Cortex 21, 2565–2577.
Sporns, O., Honey, C.J., Kotter, R., 2007. Identification and classification of hubs in brain networks. PLoS One 2, e1049.
Tournier, J.D., Mori, S., Leemans, A., 2011. Diffusion tensor imaging and beyond. Magnetic Resonance in Medicine 65, 1532–1556.
Toxopeus, C.M., de Vries, P.M., de Jong, B.M., Johnson, K.A., George, M.S., Bohning, D.E., Walker, J., Leenders, K.L., 2007. Cerebral activation patterns related to initiation and inhibition of hand movement. Neuroreport 18, 1557–1560.
Tuch, D.S., Reese, T.G., Wiegell, M.R., Makris, N., Belliveau, J.W., Wedeen, V.J., 2002. High angular resolution diffusion imaging reveals intravoxel white matter fiber heterogeneity. Magnetic Resonance in Medicine 48, 577–582.
Tzourio-Mazoyer, N., Landeau, B., Papathanassiou, D., Crivello, F., Etard, O., Delcroix, N., Mazoyer, B., Joliot, M., 2002. Automated anatomical labeling of activations in SPM using a macroscopic anatomical parcellation of the MNI MRI single-subject brain. NeuroImage 15, 273–289.
van den Heuvel, M.P., Mandl, R.C., Stam, C.J., Kahn, R.S., Hulshoff Pol, H.E., 2010. Aberrant frontal and temporal complex network structure in schizophrenia: a graph theoretical analysis. The Journal of Neuroscience 30, 15915–15926.
van Wijk, B.C.M., Stam, C.J., Daffertshofer, A., 2010. Comparing brain networks of different size and connectivity density using graph theory. PLoS One 5, e13701.
Vandenberghe, R., Gitelman, D.R., Parrish, T.B., Mesulam, M.M., 2001. Functional specificity of superior parietal mediation of spatial shifting. NeuroImage 14, 661–673.
Vos, S.B., Jones, D.K., Viergever, M.A., Leemans, A., 2011. Partial volume effect as a hidden covariate in DTI analyses. NeuroImage 55, 1566–1576.
Vos, S.B., Jones, D.K., Jeurissen, B., Viergever, M.A., Leemans, A., 2012. The influence of complex white matter architecture on the mean diffusivity in diffusion tensor MRI of the human brain. NeuroImage 59, 2208–2216.
Wen, W., Zhu, W., He, Y., Kochan, N.A., Reppermund, S., Slavin, M.J., Brodaty, H., Crawford, J., Xia, A., Sachdev, P., 2011. Discrete neuroanatomical networks are associated with specific cognitive abilities in old age. The Journal of Neuroscience 31, 1204–1212.
Wheeler-Kingshott, C.A.M., Cercignani, M., 2009. About "axial" and "radial" diffusivities. Magnetic Resonance in Medicine 61, 1255–1260.
Yantis, S., Schwarzbach, J., Serences, J.T., Carlson, R.L., Steinmetz, M.A., Pekar, J.J., Courtney, S.M., 2002. Transient neural activity in human parietal cortex during spatial attention shifts. Nature Neuroscience 5, 995–1002.
Zalesky, A., Fornito, A., Bullmore, E.T., 2010. Network-based statistic: identifying differences in brain networks. NeuroImage 53, 1197–1207.